Cholesterol Hydroperoxides Generate Singlet Molecular Oxygen [O 2 (1 Δ g)]: Near-IR Emission, 18 O-Labeled Hydroperoxides, and Mass Spectrometry

ARTICLE *in* CHEMICAL RESEARCH IN TOXICOLOGY · JUNE 2011

Impact Factor: 3.53 · DOI: 10.1021/tx200079d · Source: PubMed

7 AUTHORS, INCLUDING:

Graziella E Ronsein
University of São Paulo
24 PUBLICATIONS **394** CITATIONS
SEE PROFILE

Fernanda Manso Prado
University of São Paulo
32 PUBLICATIONS **506** CITATIONS
SEE PROFILE

Sayuri Miyamoto
University of São Paulo
79 PUBLICATIONS **1,247** CITATIONS
SEE PROFILE

Paolo Di Mascio
University of São Paulo
237 PUBLICATIONS **7,278** CITATIONS
SEE PROFILE

Chemical Research in Toxicology

ARTICLE

pubs.acs.org/crt

Cholesterol Hydroperoxides Generate Singlet Molecular Oxygen [O_2 ($^1\Delta_g$)]: Near-IR Emission, ^{18}O-Labeled Hydroperoxides, and Mass Spectrometry

Miriam Uemi, Graziella E. Ronsein, Fernanda M. Prado, Flávia D. Motta, Sayuri Miyamoto, Marisa H. G. Medeiros, and Paolo Di Mascio*

Departamento de Bioquímica, Instituto de Química, Universidade de São Paulo, CEP 05513-970, CP26077, São Paulo, SP, Brazil

Supporting Information

ABSTRACT: In mammalian membranes, cholesterol is concentrated in lipid rafts. The generation of cholesterol hydroperoxides (ChOOHs) and their decomposition products induces various types of cell damage. The decomposition of some organic hydroperoxides into peroxyl radicals is known to be a potential source of singlet molecular oxygen [O_2 ($^1\Delta_g$)] in biological systems. We report herein on evidence of the generation of O_2 ($^1\Delta_g$) from ChOOH isomers in solution or in liposomes containing ChOOHs, which involves a cyclic mechanism from a linear tetraoxide intermediate originally proposed by Russell. Characteristic light emission at 1270 nm, corresponding to O_2 ($^1\Delta_g$) monomolecular decay, was observed for each ChOOH isomer or in liposomes containing ChOOHs. Moreover, the presence of O_2 ($^1\Delta_g$) was unequivocally demonstrated using the direct spectral characterization of near-infrared light emission. Using ^{18}O-labeled cholesterol hydroperoxide (Ch^{18}O^{18}OH), we observed the formation of ^{18}O-labeled O_2 ($^1\Delta_g$) [$^{18}O_2$ ($^1\Delta_g$)] by the chemical trapping of $^{18}O_2$ ($^1\Delta_g$) with 9,10-diphenylanthracene (DPA) and detected the corresponding ^{18}O-labeled DPA endoperoxide (DPA^{18}O^{18}O) and the ^{18}O-labeled products of the Russell mechanism using high-performance liquid chromatography coupled to tandem mass spectrometry. Photoemission properties and chemical trapping clearly demonstrate that the decomposition of Ch^{18}O^{18}OH generates $^{18}O_2$ ($^1\Delta_g$), which is consistent with the Russell mechanism and points to the involvement of O_2 ($^1\Delta_g$) in cholesterol hydroperoxide-mediated cytotoxicity.

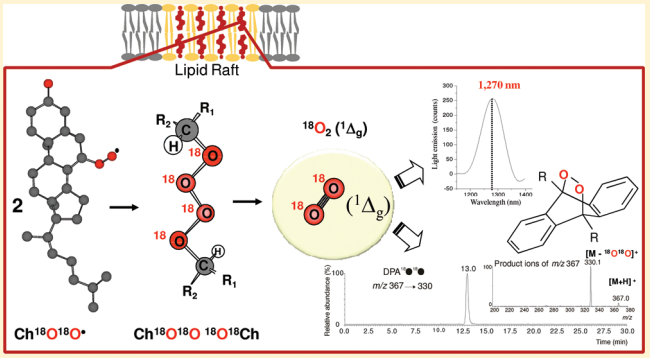

INTRODUCTION

Cholesterol is a neutral lipid found in all mammalian membranes and is especially concentrated in lipid rafts. Lipid rafts are subdomains of the plasma membrane that contain high concentrations of cholesterol and glycosphingolipids.[1] Cholesterol, as an unsaturated lipid, is also susceptible to oxidation in the presence of reactive oxygen species (ROS), giving rise to mutagenic and cytotoxic products.[2,3] Cholesterol hydroperoxides (ChOOHs) are the first oxidation products formed during cholesterol photooxidation[4−9] and lipid peroxidation.[10,11] The generation of ChOOH and its decomposition products in lipid rafts can affect the binding of signaling molecules, receptors, and proteins.[12,13] These molecules can be targets of ROS produced through ChOOH decomposition, leading to the loss of function or altered signaling pathways. Thus, the identification of ChOOHs provides important insights into the role ROS plays in biological damage.[14−18]

Singlet molecular oxygen [O_2 ($^1\Delta_g$)] in its first excited state, denoted as O_2 ($^1\Delta_g$), exhibits a substantial reactivity toward electron-rich organic molecules, leading to the formation of allylic hydroperoxides, dioxetanes, or endoperoxides.[19,20] Singlet oxygen has been shown to be generated in biological systems.[21,22] As possible biological sources of O_2 ($^1\Delta_g$), some examples include enzymatic processes catalyzed by peroxidases or oxygenases, reactions of hydrogen peroxide with hypochlorite or peroxynitrite, and the thermodecomposition of dioxetanes, endoperoxides, and type II photosensitization reactions.[23−29] UV irradiation of aromatic amino acids in protein immunoglobulins is responsible for the production of O_2 ($^1\Delta_g$).[30−33] The presence of a pair of electrons with opposite spin in the highest occupied molecular orbital confers dienophilic properties to the O_2 ($^1\Delta_g$), which explains its substantial reactivity toward electron-rich organic molecules, particularly with those exhibiting conjugated double bonds.[19,20] The reactions of O_2 ($^1\Delta_g$) with unsaturated fatty acids, proteins, and DNA have been extensively studied since this activated oxygen species can induce various types of cell damage related to aging, cancer, and other cytotoxic effects.[34]

Received: February 18, 2011

   dx.doi.org/10.1021/tx200079d | *Chem. Res. Toxicol.* XXXX, XXX, 000–000

Scheme 1. Chemical Trapping of $^{16}O_2$ ($^1\Delta_g$) and ^{18}O-Labeled O_2 ($^1\Delta_g$) by DPA To Form the Stable Corresponding Anthracene Endoperoxide DPA^{x}O^{x}O (x = 16 or 18)

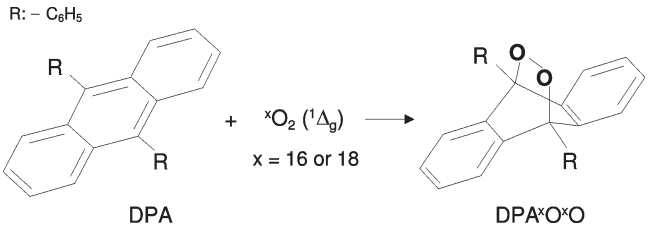

It is well-known that lipid hydroperoxides can generate singlet molecular oxygen through the self-reaction of peroxyl radicals via the Russell mechanism.[35−38] To study the possibility of ChOOHs generating O_2 ($^1\Delta_g$), photooxidation of cholesterol was performed, and ChOOHs 3β-hydroxicholest-5-ene-7α-hydroperoxide (7α-OOH), 3β-hydroxycholest-4-ene-6β-hydroperoxide (6β-OOH), and 3β-5α-cholest-6-ene-5-hydroperoxide (5α-OOH) were isolated and purified by high-performance liquid chromatography (HPLC).[39−41] O_2 ($^1\Delta_g$) was measured using chemiluminescence, which showed that ChOOHs are able to produce O_2 ($^1\Delta_g$) in the presence of cerium ions (Ce^{4+}). Moreover, the reaction of ChOOHs with Ce^{4+} produced an alcohol and a ketone, two products formed via the Russell mechanism, which were detected by high-pressure liquid chromatography coupled to tandem mass spectrometry (HPLC/MS/MS). Additionally, ^{18}O-labeled O_2 ($^1\Delta_g$) [$^{18}O_2$ ($^1\Delta_g$)] was also observed by chemical trapping with 9,10-diphenylanthracene (DPA) in a two phase $CHCl_3/D_2O$, generating the corresponding ^{18}O-labeled DPA endoperoxide (DPA^{18}O^{18}O) (Scheme 1), detectable by HPLC/MS/MS.

MATERIAL AND METHODS

Materials. Cholesterol (cholest-5-en-3β-ol) was obtained from Sigma (St. Louis, MO). Silica gel 60 (230−400 mesh), ammonium cerium(IV) nitrate, dimyristoylphosphatidylcholine (DMPC), DPA, 9,10-dibromoanthracene (DBA), and sodium azide were purchased from Aldrich (Steinheim, Germany). The $^{18}O_2$ gas cylinder (99% ^{18}O) was from Isotec-Sigma (St. Louis, MO). Deuterium oxide (D_2O) was acquired from Cambridge Isotope Laboratories (Rio de Janeiro, Brazil). Silica gel 60 F_{254} plates, methylene blue, and solvents of HPLC grade were acquired from Merck (Rio de Janeiro, Brazil). The water used in the experiments was treated with the Nanopure Water System (Barnstead, Dubuque, IA). The 1,4-dimethylnaphthalene endoperoxide ($DMNO_2$) was synthesized as described by Di Mascio et al.[42]

Synthesis and Purification of ChOOHs. ChOOHs (7α-OOH, 5α-OOH, and 6β-OOH) were synthesized by photooxidation of cholesterol using methylene blue as a sensitizer. Two hundred milligrams of cholesterol was dissolved in 20 mL of chloroform containing 10 μM methylene blue, prepared in methanol. The solution under continuous stirring and oxygen-saturated atmosphere was cooled at 4 °C and irradiated using two tungsten lamps (500 W) for 2.5 h. The ChOOHs were purified by silica gel 60 column (230−400 mesh). The column was equilibrated with hexane, and then, a gradient of hexane and ethyl ether was used. The ChOOHs were analyzed by thin-layer chromatography (TLC) using Merck 0.25 mm coated silica gel 60 F_{254} plates. The TLC plate was eluted with ethyl acetate and isooctane (1:1, v/v).

The ChOOH isomers were purified using a Shimadzu HPLC system (Tokyo, Japan), and a 250 mm × 10 mm (particle size, 5 μm) ODS column (ThermoQuest) (Supporting Information, Figure S1). The mobile phase was acetonitrile, water, and methanol (90:8:2, v/v/v), and compounds were eluted in isocratic mode at flow rate of 3.6 mL/min. The UV detector was set at 210 nm.[7] The quantification of each isolated ChOOH was done using the iodometric method described by Girotti et al.[43] and Thomas et al.[44]

Synthesis and Purification of ^{18}O-Labeled Cholesterol Hydroperoxide (Ch^{18}O^{18}OHs). Photooxidation of cholesterol (51.7 mM dissolved in chloroform) in an $^{18}O_2$-saturated atmosphere was performed in the presence of methylene blue (0.2 mM in methanol).[41] Irradiation was carried out in an ice bath for 3 h using light from a tungsten lamp (500 W). The oxygen contained in the system was removed by successive freezing and thawing under vacuum. This procedure was repeated at least five times to ensure complete removal of $^{16}O_2$. Thereafter, the whole system was connected to an $^{18}O_2$ gas cylinder under 0.5 atm. Cholesterol-oxidized products generated by photosensitization, namely, 7α-OOH, 5α-OOH, 6α-OOH, 6β-OOH, and 3β-hydroxy-5β-hydroxy-B-norcholestane-6β-carboxaldehyde (ChAld), were purified by TLC and HPLC according to Ronsein et al.[41] HPLC coupled to dopant-assisted atmospheric pressure photoionization (APPI) tandem mass spectrometry of ChOOH and ChAld was performed in an Agilent HPLC system (1200 series, Waldbronn, Germany) connected to a 4000 Q Trap mass spectrometer with an APPI source (Applied Biosystems, Foster City, CA) (Supporting Information, Figure S2).[41]

Monomol Light Emission Measurements of O_2 ($^1\Delta_g$). Monomol light emission of O_2 ($^1\Delta_g$) at 1270 nm was monitored during the reaction of ChOOH mixture or each isolated ChOOH and Ce^{4+} ions. For this assay, the Ce^{4+} solution (final concentration, 3.1 mM, prepared in D_2O) was infused into a quartz cuvette containing a ChOOH (final concentration, 9.4 mM in ethanol) at a flow rate of 0.6 mL/min.

For the acquisition of monomol light emission spectrum of O_2 ($^1\Delta_g$), Ce^{4+} ions (final concentration, 6 mM in D_2O) was infused at flow rate of 0.6 mL/min into a mixture of ChOOH (final concentration, 5.4 mM). As a reference, the spectrum of O_2 ($^1\Delta_g$) produced in the reaction of H_2O_2 and HOCl and $DMNO_2$ was also acquired. For H_2O_2 and HOCl reaction, HOCl was infused into H_2O_2 solution (final concentration, 0.28 and 1 M, respectively) at a flow rate of 1.4 mL/min and for $DMNO_2$, a 60 mM concentration of the endoperoxide in methanol was incubated at 40 °C.

HPLC/MS/MS Analysis of Products Generated in the Reaction of ChOOH and Ce^{4+} Ions. The products generated in the reaction of ChOOHs (7α-OOH, 5α-OOH, and 6β-OOH) and Ce^{4+} ions were analyzed by a Shimadzu HPLC system (Tokyo, Japan) coupled to a triple-quadrupole mass spectrometer (Quattro II, Micromass, Altricham, United Kingdom) (HPLC/MS/MS) (Supporting Information, Figures S3 and S4).

For HPLC/MS/MS analysis, 30 μL of the reaction mixture was injected into a Shimadzu C18 column (250 mm × 4.6 mm, 5 μm particle size) and eluted in isocratic mode with acetonitrile and 1% ammonium formate (91:9, v/v) as the solvent. The flow rate was 1.5 mL/min. The column oven and UV detector were set at 25 °C and 210 nm, respectively. The analysis in the mass spectrometer was performed using positive atmospheric pressure chemical ionization source ($APCI^+$). The mass spectrometer parameters were as follows: source temperature, 150 °C; APCI probe temperature, 400 °C; sample cone voltage, 25 V; extractor cone voltage, 5 V; corona potential, 3.5 kV; and collision energy, 15 eV. The flow rates of drying and nebulizing gases were 400 and 30 L/h, respectively. The HPLC/MS/MS detection of alcohol (ChOH) and ketone (ChKeto) was performed by SRM (selected reaction monitoring) mode by monitoring the mass transition of m/z 385 → 383 for ChOH and m/z 401 → 383 for ChKeto.

dx.doi.org/10.1021/tx200079d |Chem. Res. Toxicol. XXXX, XXX, 000–000

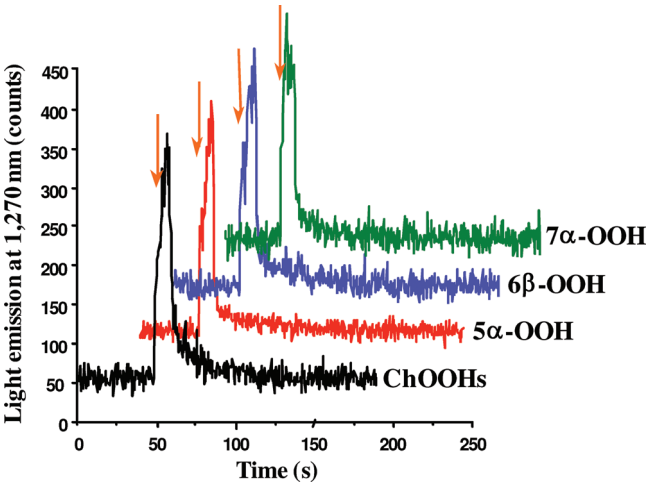

Figure 1. Monomol light emission of O_2 ($^1\Delta_g$) at 1270 nm generated in reactions containing a mixture of ChOOHs (ChOOHs) or the isolated isomers (5α-, 6β-, and 7α-OOH). Arrows indicate the injection of Ce^{4+} solution.

Chemical Trapping of O_2 ($^1\Delta_g$) and HPLC Analysis of the Reaction ChOOH/Ce^{4+}/DPA. Evidence of O_2 ($^1\Delta_g$) generation in the reaction ChOOH and Ce^{4+} was obtained by chemical trapping of O_2 ($^1\Delta_g$) with DPA, being the corresponding endoperoxide [9,10-diphenylanthracene endoperoxide ($DPAO_2$)] detected by HPLC (Supporting Information, Figure S5). For this assay, 50 μL of each isolated ChOOH (final concentration, 25 mM in chloroform) and 50 μL of DPA (final concentration, 60 mM in chloroform) were reacted in a glass tube that was protected from light. Following, 100 μL of Ce^{4+} ions was added (final concentration, 25 mM in D_2O), and the reaction was incubated at 37 °C during 1 h with string (1300 rpm). After incubation, 20 μL of the organic phase was removed and dried with nitrogen gas, and 200 μL of acetone was added to the residue. An aliquot of 50 μL was separated and mixed with 50 μL of NaN_3 [final concentration, 20 mM in H_2O/acetonitrile (10:90, (v/v)] and 25 μL of DBA (final concentration, 0.2 mM in acetonitrile).

$DPAO_2$ (30 μL of incubation) was analyzed through a Shimadzu C18 column (250 mm × 4.6 mm, 5 μm particle size), using 1% ammonium formate (solvent A) and acetonitrile (solvent B) as the mobile phase using the following linear gradient: 75−100% B in 15 min, 100% B for 10 min, 100−75% B in 5 min, and 75% until 40 min. The flow rate and UV detector were set at 1 mL/min and 210 nm, respectively.

Chemical Trapping of $^{18}O_2$ ($^1\Delta_g$) and HPLC/MS/MS Analysis of the Reaction $Ch^{18}O^{18}OHs/Ce^{4+}$/DPA. ^{18}O-Labeled O_2 ($^1\Delta_g$) can be produced in the reaction of $Ch^{18}O^{18}OHs$ and Ce^{4+}. The generation of $^{18}O_2$ ($^1\Delta_g$) was confirmed by chemical trapping of $^{18}O_2$ ($^1\Delta_g$) using DPA. $DPA^{18}O^{18}O$ and $DPA^{18}O^{16}O$ were detected by HPLC/MS/MS in the SRM mode (m/z 367 → 330 for $DPA^{18}O^{18}O$ and m/z 365 → 330 for $DPA^{18}O^{16}O$). Besides ^{18}O-labeled DPA endoperoxides, it was possible to observe the formation of unlabeled DPA endoperoxide ($DPA^{16}O^{16}O$, m/z 363 → 330).

The HPLC/MS/MS analysis were performed using the same system described for ChOOH analysis. For analytical purposes a Phenomenex Gemini C-18 column (250 mm × 4.6 mm i.d., 5 μm particle size) was used, and the UV detector was set to 210 nm. The samples were analyzed using 0.1% formic acid as solvent A and acetonitrile as solvent B, with a flow rate of 0.8 mL/min. The linear gradient was 75−100% B for 10 min, 100% B for 10 min, 100−75% B during 2 min, and 75% B until 30 min. The flux of 0.25 mL/min was directed to the mass spectrometer from 10 to 15 min, using a FCV-12AH Shimadzu valve. Mass spectrometry parameters were set at source temperature of 150 °C, APCI probe temperature of 300 °C, sample cone voltage of 15 V, extractor cone voltage of 4 V, corona potential of 3.5 kV, and collision energy of 15 eV. The flow rates of drying and nebulizing gases were 400 and 30 L/h, respectively.

A mixture of $Ch^{18}O^{18}OHs$ (final concentration, 20 mM in chloroform) was reacted with DPA (final concentration, 60 mM in chloroform) and Ce^{4+} ions (final concentration, 20 mM in D_2O). The reaction was protected from light and maintained at 37 °C during 15 min under stirring (1300 rpm). After that, 20 μL of reaction was dried with nitrogen gas, and the residue was dissolved in 50 μL of acetone. From this solution, 40 μL was mixed with 40 μL of acetonitrile. Finally, an aliquot of 70 μL was injected into the HPLC/MS/MS system.

Preparation of Liposomes Containing ChOOH. Liposomes of defined size (100 nm) were prepared by an extrusion technique.[45] Briefly, a solution containing ChOOH mixture (2 mM, final concentration) and DMPC (2 mM, final concentration) in ethanol was dried under nitrogen atmosphere and by vacuum. Then, 1 mL of D_2O was added. The solution was mixed vigorously for 1 min and extruded 21 times through a 100 nm polycarbonate membrane filter using the Liposofast kit (Avestin Inc., Ontario, Canada).

RESULTS

The chemiluminescence studies provided important information about the excited species generated during the reaction. This method is used for the detection and characterization of the radioactive monomol transition of O_2 ($^1\Delta_g$) to its ground state ($^1\Delta_g \rightarrow {}^3\Sigma_g^-$) in the near-infrared region (NIR) at 1270 nm (eq 1).[37,38,46]

$$O_2(^1\Delta_g) \rightarrow O_2(^3\Sigma_g^-) + h\nu\ (\lambda = 1270\ \text{nm}) \qquad (1)$$

Monomol light emission of O_2 ($^1\Delta_g$) was measured for the mixture of ChOOHs and each isolated ChOOH, using a special photon counting apparatus developed in our laboratory.[37,38] For the assay, Ce^{4+} (final concentration, 3.1 mM in D_2O) was infused into a quartz cuvette containing a mixture of ChOOHs or the isolated isomers (5α-, 6β-, and 7α-OOH) (final concentration, 9.4 mM in ethanol) at a flow rate of 0.6 mL/min. The injection of Ce^{4+} into the solution produced an intense monomol light emission signal, generated by the monomolecular decay of O_2 ($^1\Delta_g$) (Figure 1).

In addition, the monomol light emission spectrum of O_2 ($^1\Delta_g$) produced in the reaction containing the ChOOH mixture and Ce^{4+} was also confirmed by recording the spectrum of the light emitted in the NIR (Figure 2A). For comparative purposes, the spectrum of the O_2 ($^1\Delta_g$) generated by the reaction of H_2O_2 with HOCl[47−50] (eq 2, Figure 2B) and by $DMNO_2$ thermodecomposition (eq 3, Figure 2C) was also acquired (eq 2).

$$H_2O_2 + OCl^- \rightarrow H_2O + HOCl + O_2(^1\Delta_g)\ (100\%) \qquad (2)$$

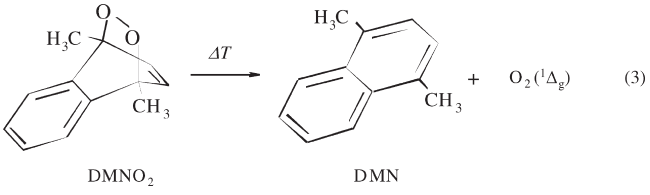

(3)

All spectra showed an emission band with a maximum intensity at 1270 nm, characteristic of O_2 ($^1\Delta_g$) monomolecular

dx.doi.org/10.1021/tx200079d |Chem. Res. Toxicol. XXXX, XXX, 000–000

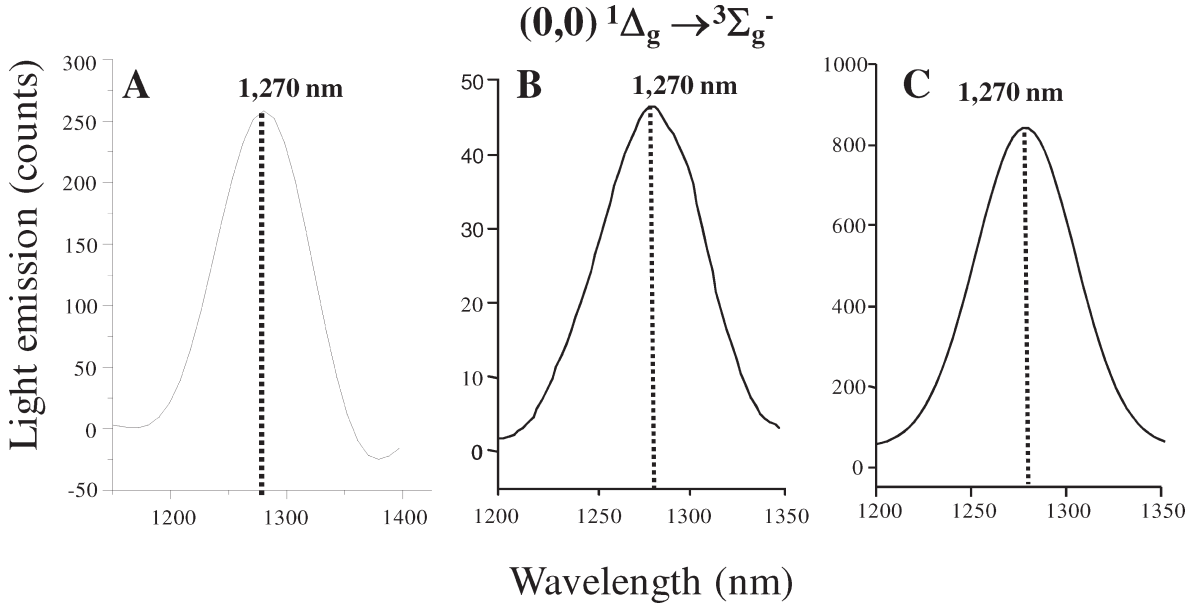

Figure 2. NIR monomol light emission spectrum of O_2 ($^1\Delta_g$) obtained from the reactions in the (A) ChOOHs/Ce^{4+}/D_2O, (B) H_2O_2/HOCl/H_2O systems, and in the thermodecomposition of $DMNO_2$.

Scheme 2. Russell Mechanism for the Self-Reaction of Cholesterol Peroxyl Radical (7Ch^{18}O^{18}O$^{\bullet}$ or 5Ch^{18}O^{18}O$^{\bullet}$), Generating $^{18}O_2$ ($^1\Delta_g$), 5-Ch^{18}OH, 7-Ch^{18}OH, and 7-Ch^{18}O Keto

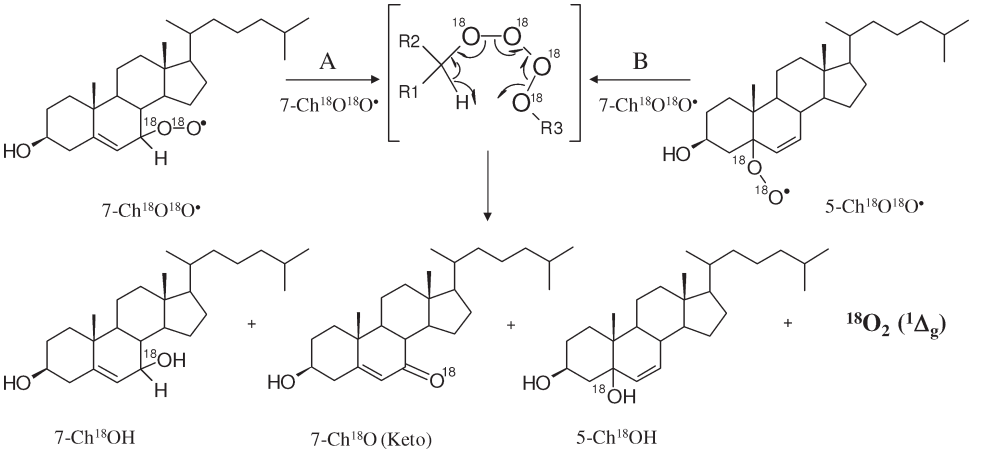

decay and, thus, clearly demonstrating that O_2 ($^1\Delta_g$) was formed in the reaction of ChOOHs with Ce^{4+}. Further evidence that the light emitted in the reaction corresponds to O_2 ($^1\Delta_g$) was obtained by testing the effect of nondeuterated versus deuterated solvent and by testing the effect of sodium azide, a known O_2 ($^1\Delta_g$) quencher.[51−53] The intensity of the light emitted in the reaction conducted in buffer prepared in D_2O was higher than in the reaction conducted in buffer containing H_2O. This observation is consistent with the fact that the lifetime of O_2 ($^1\Delta_g$) is about 10 times longer in D_2O than in H_2O. The quenching effect of azide on the chemiluminescent reaction was also observed.

In previous studies, we demonstrated that the generation of O_2 ($^1\Delta_g$) using linoleic acid hydroperoxide in the presence of metal ions, peroxynitrite, and HOCl involves the Russell mechanism.[28,37,38] In this mechanism, primary or secondary peroxyl radicals react via a cyclic mechanism[35] involving a acyclic tetraoxide intermediate that decomposes to generate an alcohol, a ketone, and molecular oxygen (Scheme 2). This reaction may generate either O_2 ($^1\Delta_g$) or an electronically excited ketone.[35,36] In fact, it was shown that the generation of O_2 ($^1\Delta_g$) is favored over the electronically excited ketone.[54]

To investigate the mechanism involved in the generation of O_2 ($^1\Delta_g$) by ChOOH, the products formed in the reaction of a 2 mM ChOOH isomer (7α-, 6β-, and 5α-OOH) with 2 mM Ce^{4+} ions in D_2O at 37 °C with 5 min of vigorous mixing were analyzed by HPLC/MS/MS using the APCI source in the positive mode. The UV detector connected to the system was set at 210 nm. The HPLC/MS/MS analyses were performed in the SRM mode by monitoring the loss of one or two water molecules from the ketone (m/z 401 → 383, peak at

dx.doi.org/10.1021/tx200079d |*Chem. Res. Toxicol.* XXXX, XXX, 000–000

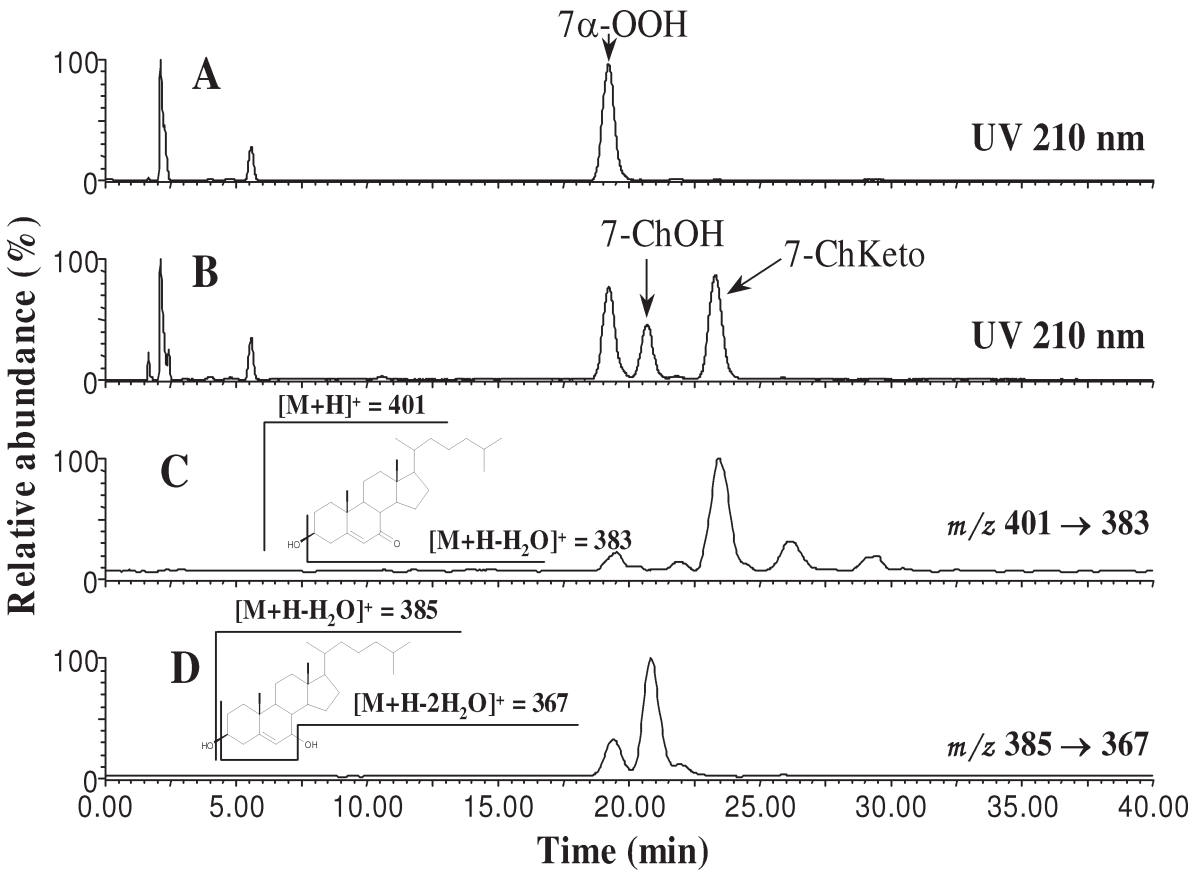

Figure 3. HPLC/MS/MS detection of the products generated in the reaction of 7α-OOH and Ce^{4+}. UV chromatogram at 210 nm of 7α-OOH (A) and the reaction of 7α-OOH with Ce^{4+} (B). SRM chromatograms of the mass transition: m/z 401 → 383 (C) and m/z 385 → 367 (D).

23.3 min, Figure 3C) and the alcohol (m/z 385 → 367, peak at 20.7 min, Figure 3D), respectively.

The results obtained from the reaction of 7α-OOH and Ce^{4+} are shown in Figure 3. The UV chromatogram at 210 nm shows two peaks, one corresponds to the alcohol 7-ChOH and the other to the ketone 7-ChKeto (Figure 3B), beyond the peak of 7α-OOH (Figure 3A) (see the Supporting Information, Figure S6).

The results obtained from the reaction of isomer 6β-OOH and Ce^{4+} also showed the formation of the corresponding ketone and alcohol products (see the Supporting Information, Figures S3 and S4), the two characteristic products of the Russell mechanism. Yet, analysis of the 5α-OOH/Ce^{4+} reaction showed a different pattern of products (Figure 4). Before the reaction, the UV chromatogram (Figure 4A) showed one major peak, corresponding to the 5α-OOH at 21.8 min and another minor peak with the same retention time for 7α-OOH at 19.5 min (Figure 3A). After the reaction, four peaks were detected (Figure 4B) and the SRM analysis demonstrated that two of these had the same retention time as did the 7α-OOH decomposition products (7-ChOH at m/z 385 → 367, Figure 4C, and 7-ChKeto at and m/z 401 → 383, Figure 4D). The peak at 22.0 min (Figure 4C) corresponds to a 5α-OOH decomposition product, 5α-hydroxycholest-6-ene (5-ChOH at m/z 385 → 367). In the chromatogram in Figure 4D, the peak at 21.8 min corresponds to the residual 5α-OOH, which has the same SRM mass transition of 7-ChKeto (m/z 401 → 383) and thus represents the loss of two water molecules from 5α-OOH. The peak at 26.0 min (Figure 4D) can be attributed to 7β-ketonecholestan, generated by a dissociative mechanism from 7α-OOH to 7β-OOH, as previously described by Beckwith et al.[55]

The generation of O_2 ($^1\Delta_g$) was also confirmed through the detection of $^{18}O_2$ ($^1\Delta_g$) formed in the reaction of ^{18}O-labeled ChOOHs ($Ch^{18}O^{18}OHs$; final concentration, 20 mM in ethanol) with Ce^{4+} (final concentration, 20 mM in D_2O). ^{18}O-labeled O_2 ($^1\Delta_g$) was chemically trapped with DPA (final concentration, 60 mM in chloroform), and the corresponding ^{18}O-labeled DPA endoperoxide (Scheme 1) was detected by HPLC/MS/MS (Figure 5). The formation of $DPAO_2$ was observed through monitoring the mass transition of unlabeled DPA endoperoxide ($DPA^{16}O^{16}O$, m/z 363 → 330, Figure 5A) and the mass transition of $DPA^{18}O^{18}O$ (m/z 367 → 330, Figure 5B and ($DPA^{18}O^{16}O$, m/z 365 → 330, Figure 5C). The fragment ion spectrum at m/z 363 ($DPA^{16}O^{16}O$, Figure 5A inset), m/z 367 ($DPA^{18}O^{18}O$, Figure 5B inset), and m/z 365 ($DPA^{18}O^{16}O$, Figure 5C inset) shows an intense fragment ion at m/z 330 that corresponds to the lost of molecular oxygen from the $DPA^{x}O^{x}O$ (Scheme 1) molecule. The DPA endoperoxide with one ^{18}O isotopically labeled oxygen atom ($DPA^{18}O^{16}O$, m/z 365 → 330) was also detected by HPLC/MS/MS (Figure 5C). Detection of $DPA^{18}O^{18}O$ (m/z 367 → 330, Figure 5B) clearly demonstrated the generation of $^{18}O_2$ ($^1\Delta_g$) that occurs by the self-reaction of two ^{18}O-labeled peroxyl radicals of ChOOH ($Ch^{18}O^{18}O^{\bullet}$) (Scheme 2). The formation of $^{16}O_2$ ($^1\Delta_g$) and detection of

dx.doi.org/10.1021/tx200079d |*Chem. Res. Toxicol.* XXXX, XXX, 000–000

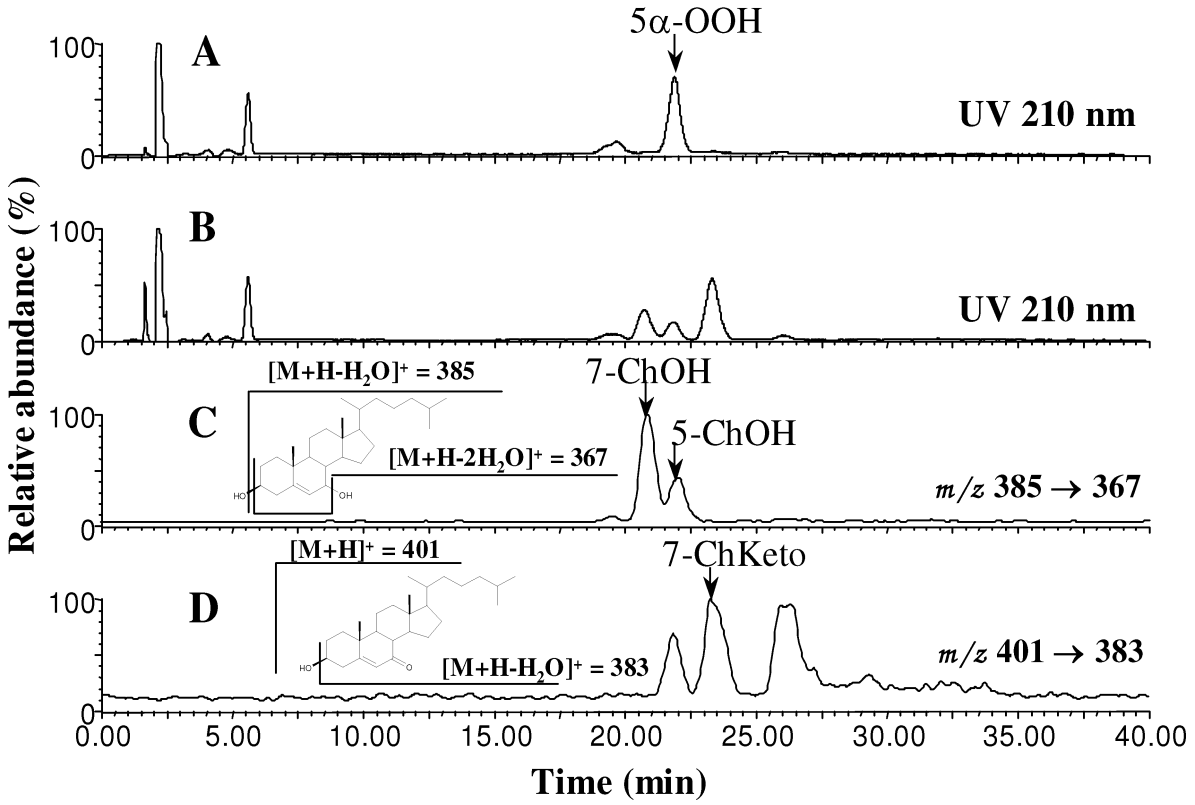

Figure 4. HPLC/MS/MS detection of the products generated in the reaction of 5α-OOH and Ce^{4+}. UV chromatogram at 210 nm of 5α-OOH (A) and reaction of 5α-OOH with Ce^{4+} (B). SRM chromatogram of the mass transition: m/z 385 → 367 (C) and m/z 401 → 383 (D).

DPA^{16}O^{16}O could be (i) related to a reaction between two unlabeled peroxyl radicals (Ch^{16}O^{16}O$^{\bullet}$) generated from residual unlabeled ChOOHs (12.5%)[37] or derived from the replacement of $^{18}O_2$ from the peroxyl moiety of Ch^{18}O^{18}O$^{\bullet}$ to $^{16}O_2$ dissolved in the reaction system,[56] (ii) due to an energy transfer mechanism from $^{18}O_2$ ($^1\Delta_g$) to $^{16}O_2$ in the fundamental ground state ($^3\Sigma_g^-$),[57,58] or (iii) due to the reaction of two peroxyl radicals containing only one labeled oxygen (Ch^{18}O^{16}O$^{\bullet}$), which can be formed by oxygen exchange reactions with water or molecular oxygen.[37] The detection of DPA^{18}O^{16}O is probably due to the reaction of labeled and unlabeled peroxyl radicals.

On the basis of these observations and the fact that the presence of hydrogen-α (Scheme 2) is known to be critical for the generation of O_2 ($^1\Delta_g$) by the Russell mechanism, we propose the mechanism of O_2 ($^1\Delta_g$) generation by 7α-OOH and 5α-OOH. The mechanism involved in the generation of $^{18}O_2$ ($^1\Delta_g$) by the isomer ^{18}O-labeled 7α-OOH (7α-^{18}O^{18}OH) depends on the formation of the ^{18}O-labeled 7-cholesterol peroxyl (7-Ch^{18}O^{18}O$^{\bullet}$) radical, which can react with another 7-Ch^{18}O^{18}O$^{\bullet}$ radical to generate a tetraoxide intermediate (Scheme 2A). This tetraoxide intermediate can decompose into $^{18}O_2$ ($^1\Delta_g$), ^{18}O-labeled alcohol (7-Ch^{18}OH), and ^{18}O-labeled ketone (7-Ch^{18}OKeto) (Scheme 2).

In the case of ^{18}O-labeled 5α-OOH (5α-^{18}O^{18}OH), this isomer can suffer sigmatropic rearrangement into the isomer 7α-^{18}O^{18}OH,[55] which can be oxidized to the 7-Ch^{18}O^{18}O$^{\bullet}$ radical and also generate $^{18}O_2$ ($^1\Delta_g$) via the Russell mechanism. Additionally, the ^{18}O-labeled 5-cholesterol peroxyl (5-Ch^{18}O^{18}O$^{\bullet}$) radical may react with another labeled 7-Ch^{18}O^{18}O$^{\bullet}$ radical, yielding $^{18}O_2$ ($^1\Delta_g$), ^{18}O-labeled 5α-hydroxycholestan-6-ene (5-Ch^{18}OH), and 7-Ch^{18}OKeto (Scheme 2B).

To investigate the biological relevance of these data, we incorporated pure ChOOH as a mixture of ChOOHs into a unilamellar liposome. The liposome was prepared using an extrusion method.[45] For the liposome, 2 mM ChOOHs were incorporated into 2 mM DMPC in D_2O. Chemiluminescence assays were performed using the same instrument as mentioned above. For the reaction, Ce^{4+} (final concentration, 8.3 mM in ethanol) was injected into a 1.5 mL of liposome solution containing ChOOHs and DMPC in D_2O (final concentration, 2 mM) (Figure 6). In this system, O_2 ($^1\Delta_g$) generation is detected by an intense monomol light emission of O_2 ($^1\Delta_g$) at 1270 nm (Figure 6A), and sodium azide (NaN_3; final concentration, 2 mM) (Figure 6B), a well-known quencher of O_2 ($^1\Delta_g$), is used to suppress emitted light. Our results show, for the first time, that ChOOHs contained in liposomes yield O_2 ($^1\Delta_g$).

In conclusion, the results provide direct evidence of O_2 ($^1\Delta_g$) generation in the self-reaction of two cholesterol peroxyl radicals via the Russell mechanism, in which two peroxyl radicals combine via a cyclic mechanism, generating O_2 ($^1\Delta_g$), an alcohol, and a ketone (Scheme 2). Moreover, the detection of the alcohols 7-ChOH, 5-ChOH, and the ketone 7-ChKeto as the decomposition products formed in the reaction is strong evidence for the Russell mechanism. In addition, the detection of O_2 ($^1\Delta_g$) produced in the ChOOHs/DMPC system indicated the importance of ChOOH as biological source of O_2 ($^1\Delta_g$) in causing cell damage.

dx.doi.org/10.1021/tx200079d |*Chem. Res. Toxicol.* XXXX, XXX, 000–000

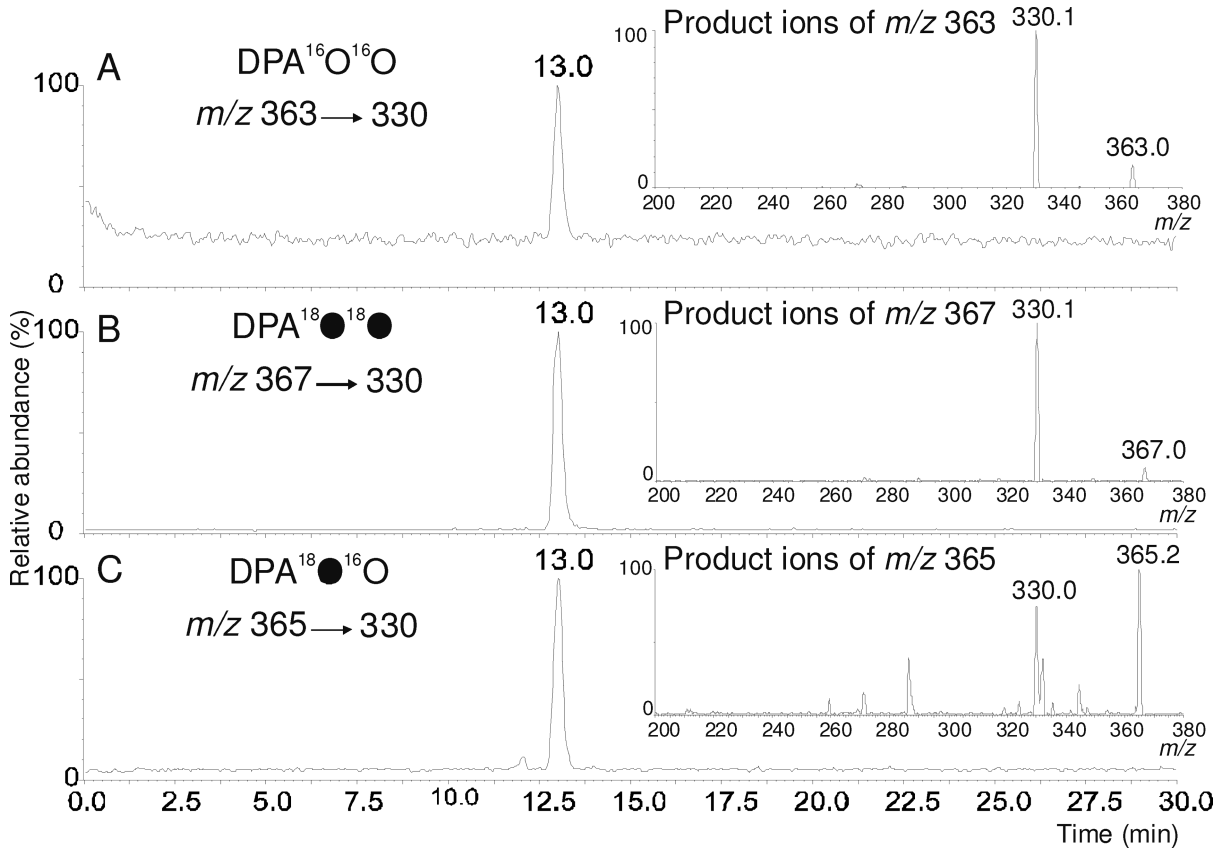

Figure 5. HPLC/MS/MS analyses of unlabeled ($DPA^{16}O^{16}O$) and labeled DPA endoperoxide ($DPA^{18}O^{18}O$ and $DPA^{18}O^{16}O$) formed in the reaction of ^{18}O-labeled ChOOHs with Ce^{4+}. Mass transition of $DPA^{16}O^{16}O$, m/z 363 → 330 (A), $DPA^{18}O^{18}O$, m/z 367 → 330 (B), and $DPA^{18}O^{16}O$, m/z 365 → 330 (C). Inset: Fragment ion spectrum of $DPA^{16}O^{16}O$ at m/z 363 (A), $DPA^{18}O^{18}O$ at m/z 367 (B), and $DPA^{18}O^{16}O$ at m/z 365 (C).

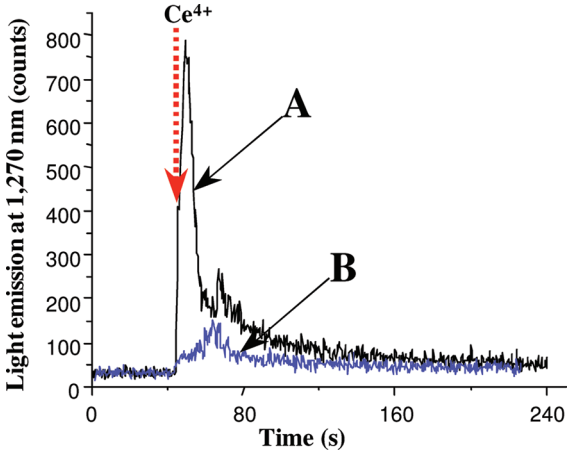

Figure 6. NIR monomol light emission of O_2 ($^1\Delta_g$) at 1270 nm generated by ChOOHs incorporated in DMPC unilamellar liposomes. Arrows indicate the injection of Ce^{4+} into (A) ChOOHs/DMPC (1:1) and (B) ChOOHs/DMPC (1:1) and 2 mM of NaN_3.

■ ASSOCIATED CONTENT

Ⓢ Supporting Information. HPLC chromatogram of 7α-, 5α-, and 6β-OOH; SRM chromatogram and enhanced product ion mass spectra obtained in the positive APPI mode for cholesterol-oxidized products; comparative HPLC chromatograms of 7α-, 5α-, or 6β-OOH before and after reaction with Ce^{4+}; HPLC/MS/MS detection of the products generated in the reaction of 6β-OOH and Ce^{4+}; HPLC chromatogram of $DPAO_2$ produced in the reaction of 6β-OOH/Ce^{4+} and mass spectra of ketone and alcohol products formed in the reaction of 7α-OOH/Ce^{4+}. This material is available free of charge via the Internet at http://pubs.acs.org.

■ AUTHOR INFORMATION

Corresponding Author

*Tel: (+55)11-3091-8498. Fax: (+55)11-3815-5579. E-mail: pdmascio@iq.usp.br.

Funding Sources

This work was supported by the following Brazilian research funding institutions: FAPESP (Fundação de Amparo à Pesquisa do Estado de São Paulo), CNPq (Conselho Nacional para o Desenvolvimento Científico e Tecnológico), Instituto do Milênio: Redoxoma, INCT de Processos Redox em Biomedicina—Redoxoma and Pró-reitoria de Pesquisa da USP. G.E.R. and F.D.M. are recipients of FAPESP fellowship.

■ ABBREVIATIONS

ChOOH, cholesterol hydroperoxides; $Ch^{18}O^{18}OH$, ^{18}O-labeled cholesterol hydroperoxides; O_2 ($^1\Delta_g$), singlet molecular oxygen; $^{18}O_2$ ($^1\Delta_g$), ^{18}O-labeled singlet molecular oxygen; DPA, 9,10-diphenylanthracene; $DPAO_2$, 9,10-diphenylanthracene endoperoxide; $DPA^{18}O^{18}O$, ^{18}O-labeled DPA endoperoxide; DBA,

dx.doi.org/10.1021/tx200079d |Chem. Res. Toxicol. XXXX, XXX, 000–000

9,10-dibromoanthracene; ROS, reactive oxygen species; 7α-OOH, 3β-hydroxicholest-5-ene-7α-hydroperoxide; 6β-OOH, 3β-hydroxycholest-4-ene-6β-hydroperoxide; 5α-OOH, 3β-5α-cholest-6-ene-5-hydroperoxide; $DMNO_2$, 1,4-dimethylnaphthalene endoperoxide; ChAld, 3β-hydroxy-5β-hydroxy-B-norcholestane-6β-carboxaldehyde; DMPC, dimyristoylphosphatidylcholine; TLC, thin-layer chromatography; HPLC/MS/MS, HPLC-tandem mass spectrometry; APCI, atmospheric pressure chemical ionization; SRM, selected reaction monitoring; ChOH, cholesterol alcohol; ChKeto, cholesterol ketone; D_2O, deuterium oxide; NIR, near-infrared region.

REFERENCES

(1) Girotti, A. W. (1998) Lipid hydroperoxide generation, turnover, and effector action in biological systems. *J. Lipid Res. 39*, 1529–1542.

(2) Girotti, A. W. (2001) Photosensitized oxidation of membrane lipids: reaction pathways, cytotoxic effects, and cytoprotective mechanisms. *J. Photochem. Photobiol., B 63*, 103–113.

(3) Korytowski, W., Geiger, P. G., and Girotti, A. W. (1996) Enzymatic reducibility in relation to cytotoxicity for various cholesterol hydroperoxides. *Biochemistry 35*, 8670–8679.

(4) Schenck, G. O., Neumuller, O. A., and Eisfeld, W. (1958) Zur photosensibilisierten autoxydation der steroide - delta-5-steroid-7alpha-hydroperoxyde und ds.7-ketone durch allylumlagerung von delta-6-steroid-5alpha-hydroperoxyden. *Ann. Chem. Justus Liebig 618*, 202–210.

(5) Kulig, M. J., and Smith, L. L. (1973) Sterol metabolism. 25. Cholesterol oxidation by singlet molecular-oxygen. *J. Org. Chem. 38*, 3639–3642.

(6) Teng, J. I., Kulig, M. J., Smith, L. L., Kan, G., and Vanlier, J. E. (1973) Sterol Metabolism. 20. Cholesterol 7β-Hydroperoxide. *J. Org. Chem. 38*, 119–123.

(7) Korytowski, W., Bachowski, G. J., and Girotti, A. W. (1991) Chromatographic separation and electrochemical determination of cholesterol hydroperoxides generated by photodynamic action. *Anal. Biochem. 197*, 149–156.

(8) Korytowski, W., and Girotti, A. W. (1999) Singlet oxygen adducts of cholesterol: Photogeneration and reductive turnover in membrane systems. *Photochem. Photobiol. 70*, 484–489.

(9) Osada, K., and Sevanian, A. (2000) Cholesterol photodynamic oxidation by ultraviolet irradiation and cholesterol ozonization by ozone exposure. *Methods Enzymol. 319*, 188–196.

(10) Girotti, A. W. (1985) Mechanisms of lipid peroxidation. *Free Radical Biol. Med. 1*, 87–95.

(11) Korytowski, W., Bachowski, G. J., and Girotti, A. W. (1992) Photoperoxidation of cholesterol in homogeneous solution, isolated membranes, and cells—Comparison of the 5-alpha-hydroperoxides and 6-beta-hydroperoxides as indicators of singlet oxygen intermediacy. *Photochem. Photobiol. 56*, 1–8.

(12) Michel, V., and Bakovic, M. (2007) Lipid rafts in health and disease. *Biol. Cell 99*, 129–140.

(13) Pike, L. J. (2003) Lipid rafts: Bringing order to chaos. *J. Lipid Res. 44*, 655–667.

(14) Ozawa, N., Yamazaki, S., Chiba, K., Aoyama, H., Tomisawa, H., Tateishi, M., and Watabe, T. (1991) Occurrence of cholesterol 7[alpha]- and 7[beta]-hydroperoxides in rat skin as aging markers. *Biochem. Biophys. Res. Commun. 178*, 242–247.

(15) Adachi, J., Asano, M., Naito, T., Ueno, Y., and Tatsuno, Y. (1998) Chemiluminescent determination of cholesterol hydroperoxides in human erythrocyte membrane. *Lipids 33*, 1235–1240.

(16) Asano, M., Adachi, J., and Ueno, Y. (1999) Cholesterol-derived hydroperoxides in alcoholic liver disease. *Lipids 34*, 557–561.

(17) Adachi, J., Asano, M., Ueno, Y., Reilly, M., Mantle, D., Peters, T. J., and Preedy, V. R. (2000) 7 alpha- and 7 beta-hydroperoxycholest-5-en-3 beta-ol in muscle as indices of oxidative stress: Response to ethanol dosage in rats. *Alcohol.: Clin. Exp. Res. 24*, 675–681.

(18) Adachi, J., Kudo, R., Ueno, Y., Hunter, R., Rajendram, R., Want, E., and Preedy, V. R. (2001) Heart 7-hydroperoxycholesterol and oxysterols are elevated in chronically ethanol-fed rats. *J. Nutr. 131*, 2916–2920.

(19) Foote, C. S. (1979) Quenching of singlet oxygen. In *Singlet Oxygen* (Wasserman, H. H., and Murray, R. W., Eds.) pp 139−171, Academic Press, New York, United States.

(20) Frimer, A. A. (1985) *Singlet O_2*, Vols. I and II, CRC Press, Boca Raton.

(21) Steinbeck, M. J., Khan, A. U., and Karnovsky, M. J. (1993) Extracellular production of singlet oxygen by stimulated macrophages quantified using 9,10-diphenylanthracene and perylene in a polystyrene film. *J. Biol. Chem. 268*, 15649–15654.

(22) Pierlot, C., Aubry, J. M., Briviba, K., Sies, H., and Di Mascio, P. (2000) Naphthalene endoperoxides as generators of singlet oxygen in biological media. *Methods Enzymol. 319*, 3–20.

(23) Cilento, G. (1982) Electronic excitation in dark biological processes. In *Chemical and Biological Generation of Excited States* (Adam, W., and Cilento, G., Eds.) pp 278−307, Academic Press, New York, United States.

(24) Held, A. M., Halko, D. J., and Hurst, J. K. (1978) Mechanism of chlorine oxidation of hydrogen peroxide. *J. Am. Chem. Soc. 100*, 5732–5740.

(25) Di Mascio, P., Bechara, E. J. H., Medeiros, M. H. G., Briviba, K., and Sies, H. (1994) Singlet molecular oxygen production in the reaction of peroxynitrite with hydrogen peroxide. *FEBS Lett. 355*, 287–289.

(26) Briviba, K., SahaMoller, C. R., Adam, W., and Sies, H. (1996) Formation of singlet oxygen in the thermal decomposition of 3-hydroxymethyl-3,4,4-trimethyl-1,2-dioxetane, a chemical source of triplet-excited ketones. *Biochem. Mol. Biol. Int. 38*, 647–651.

(27) Foote, C. S. (1991) Definition of type I and type II photosensitized oxidation. *Photochem. Photobiol. 54*, 659–659.

(28) Miyamoto, S., Martinez, G. R., Martins, A. P. B., Medeiros, M. H. G., and Di Mascio, P. (2003) Direct evidence of singlet molecular oxygen production in the reaction of linoleic acid hydroperoxide with peroxynitrite. *J. Am. Chem. Soc. 125*, 4510–4517.

(29) Miyamoto, S., Ronsein, G. E., Correa, T. C., Martinez, G. R., Medeiros, M. H. G., and Di Mascio, P. (2009) Direct evidence of singlet molecular oxygen generation from peroxynitrate, a decomposition product of peroxynitrite. *Dalton Trans.* 5720–5729.

(30) Wentworth, A. D., Jones, L. H., Wentworth, P., Janda, K. D., and Lerner, R. A. (2000) Antibodies have the intrinsic capacity to destroy antigens. *Proc. Natl. Acad. Sci. U.S.A. 97*, 10930–10935.

(31) Wentworth, P., Jr., Jones, L. H., Wentworth, A. D., Zhu, X., Larsen, N. A., Wilson, I. A., Xu, X., Goddard, W. A., III, Janda, K. D., Eschenmoser, A., and Lerner, R. A. (2001) Antibody catalysis of the oxidation of water. *Science 293*, 1806–1811.

(32) Wentworth, P., McDunn, J. E., Wentworth, A. D., Takeuchi, C., Nieva, J., Jones, T., Bautista, C., Ruedi, J. M., Gutierrez, A., Janda, K. D., Babior, B. M., Eschenmoser, A., and Lerner, R. A. (2002) Evidence for antibody-catalyzed ozone formation in bacterial killing and inflammation. *Science 298*, 2195–2199.

(33) Chin, K. K., Trevithick-Sutton, C. C., McCallum, J., Jockusch, S., Turro, N. J., Scaiano, J. C., Foote, C. S., and Garcia-Garibay, M. A. (2008) Quantitative determination of singlet oxygen generated by excited state aromatic amino acids, proteins, and immunoglobulins. *J. Am. Chem. Soc. 130*, 6912–6913.

(34) Halliwell, B., and Gutteridge, J. M. C. (1999) *Free Radicals in Biology and Medicine*, Oxford University Press, New York, United States.

(35) Russell, G. A. (1957) Deuterium-isotope effects in the autoxidation of aralkyl hydrocarbons - mechanism of the interaction of peroxy radicals. *J. Am. Chem. Soc. 79*, 3871–3877.

(36) Howard, J. A., and Ingold, K. U. (1968) Self-reaction of sec-butylperoxy radicals. Confirmation of Russell mechanism. *J. Am. Chem. Soc. 90*, 1056–1058.

(37) Miyamoto, S., Martinez, G. R., Medeiros, M. H. G., and Di Mascio, P. (2003) Singlet molecular oxygen generated from lipid hydroperoxides by the Russell mechanism: Studies using ^{18}O-labeled

linoleic acid hydroperoxide and monomol light emission measurements. *J. Am. Chem. Soc. 125*, 6172–6179.

(38) Miyamoto, S., Martinez, G. R., Rettori, D., Augusto, O., Medeiros, M. H. G., and Di Mascio, P. (2006) Linoleic acid hydroperoxide reacts with hypochlorous acid, generating peroxyl radical intermediates and singlet molecular oxygen. *Proc. Natl. Acad. Sci. U.S.A. 103*, 293–298.

(39) Uemi, M., Ronsein, G. E., Miyamoto, S., Medeiros, M. H. G., and Di Mascio, P. (2009) Generation of cholesterol carboxyaldehyde by the reaction of singlet molecular oxygen [O_2 ($^1\Delta_g$)] as well as ozone with cholesterol. *Chem. Res. Toxicol. 22*, 875–884.

(40) Mansano, F. V., Kazaoka, R. M. A., Ronsein, G. E., Prado, F. M., Genaro-Mattos, T. C., Uemi, M., Di Mascio, P., and Miyamoto, S. (2010) Highly Sensitive Fluorescent Method for the Detection of Cholesterol Aldehydes Formed by Ozone and Singlet Molecular Oxygen. *Anal. Chem. 82*, 6775–6781.

(41) Ronsein, G. E., Prado, F. M., Mansano, F. V., Oliveira, M. C. B., Medeiros, M. H. G., Miyamoto, S., and Di Mascio, P. (2010) Detection and Characterization of Cholesterol-Oxidized Products Using HPLC Coupled to Dopant Assisted Atmospheric Pressure Photoionization Tandem Mass Spectrometry. *Anal. Chem. 82*, 7293–7301.

(42) Di Mascio, P., Bechara, E. J. H., and Rubim, J. C. (1992) Dioxygen NIR FT-Emission ($^1\Delta_g \rightarrow {}^3\Sigma_g^-$) and Raman Spectra of 1, 4-Dimethylnaphthalene Endoperoxide: A Source of Singlet Molecular Oxygen. *Appl. Spectrosc. 46*, 236–239.

(43) Girotti, A. W., Thomas, J. P., and Jordan, J. E. (1985) Lipid photooxidation in erythrocyte-ghosts—Sensitization of the membranes toward ascorbate-induced and superoxide-induced peroxidation and lysis. *Arch. Biochem. Biophys. 236*, 238–251.

(44) Thomas, J. P., Maiorino, M., Ursini, F., and Girotti, A. W. (1990) Protective action of phospholipid hydroperoxide glutathione-peroxidase against membrane-damaging lipid-peroxidation—In situ reduction of phospholipid and cholesterol hydroperoxides. *J. Biol. Chem. 265*, 454–461.

(45) Miyamoto, S., Dupas, C., Murota, K., and Terao, J. (2003) Phospholipid hydroperoxides are detoxified by phospholipase A2 and GSH peroxidase in rat gastric mucosa. *Lipids 38*, 641–649.

(46) Khan, A. U. (1981) Direct spectral evidence of the generation of singlet molecular-oxygen ($^1\Delta_g$) in the reaction of potassium superoxide with water. *J. Am. Chem. Soc. 103*, 6516–6517.

(47) Foote, C. S., Wexler, S., Ando, W., and Higgins, R. (1968) Chemistry of singlet oxygen. 4. Oxygenations with hypochlorite-hydrogen peroxide. *J. Am. Chem. Soc. 90*, 975–981.

(48) Khan, A. U., and Kasha, M. (1970) Chemiluminescence arising from simultaneous transitions in pairs of singlet oxygen molecules. *J. Am. Chem. Soc. 92*, 3293–3300.

(49) Held, A. M., Halko, D. J., and Hurst, J. K. (1978) Mechanisms of chlorine oxidation of hydrogen peroxide. *J. Am. Chem. Soc. 100*, 5732–5740.

(50) Murray, R. W. (1979) Chemical sources of singlet oxygen. In *Singlet Oxygen* (Wasserman, H. H., and Murray, R. W., Eds.) pp 59−114, Academic Press, New York, United States.

(51) Hasty, N., Merkel, P. B., Radlick, P., and Kearns, D. R. (1972) Role of azide in singlet oxygen reactions—Reaction of azide with singlet oxygen. *Tetrahedron Lett.* 49–52.

(52) Merkel, P. B., and Kearns, D. R. (1972) Remarkable solvent effects on the lifetime of $^1\Delta_g$ oxygen. *J. Am. Chem. Soc. 94*, 1029–1030.

(53) Kajiwara, T., and Kearns, D. R. (1973) Direct spectroscopic evidence for a deuterium solvent effect on lifetime of singlet oxygen in water. *J. Am. Chem. Soc. 95*, 5886–5890.

(54) Niu, Q. J., and Mendenhall, G. D. (1992) Yields of singlet molecular oxygen from peroxyl radical termination. *J. Am. Chem. Soc. 114*, 165–172.

(55) Beckwith, A. L. J., Davies, A. G., Davison, I. G. E., Maccoll, A., and Mruzek, M. H. (1989) The mechanisms of the rearrangements of allylic hydroperoxides - 5-alpha-hydroperoxy-3-beta-hydroxycholest-6-ene and 7-alpha-hydroperoxy-3-beta-hydroxycholest-5-ene. *J. Chem. Soc., Perkin Trans. 2*, 815–824.

(56) Chan, H. W. S., Levett, G., and Matthew, J. A. (1979) Mechanism of the rearrangement of linoleate hydroperoxides. *Chem. Phys. Lipids 24*, 245–256.

(57) Jones, I. T. N., and Bayes, K. D. (1972) Electronic energy fransfer from $^{32}O_2(a\,^1\Delta_g)$ to $^{36}O_2(X^3\Sigma_g^-)$. *J. Chem. Phys. 57*, 1003–1004.

(58) Martinez, G. R., Ravanat, J. L., Cadet, J., Miyamoto, S., Medeiros, M. H. G., and Di Mascio, P. (2004) Energy transfer between singlet ($^1\Delta_g$) and triplet ($^3\Sigma_g^-$) molecular oxygen in aqueous solution. *J. Am. Chem. Soc. 126*, 3056–3057.